Nucl Med Mol Imaging (2013) 47:232–241
DOI 10.1007/s13139-013-0216-6

ORIGINAL ARTICLE

Heterogeneity Analysis of ^{18}F-FDG Uptake in Differentiating Between Metastatic and Inflammatory Lymph Nodes in Adenocarcinoma of the Lung: Comparison with Other Parameters and its Application in a Clinical Setting

Hendra Budiawan · Gi Jeong Cheon · Hyung-Jun Im · Soo Jin Lee · Jin Chul Paeng · Keon Wook Kang · June-Key Chung · Dong Soo Lee

Received: 19 May 2013 / Revised: 7 July 2013 / Accepted: 11 July 2013 / Published online: 21 August 2013

Abstract
Purpose Lymph node (LN) characterization is crucial in determining the stage and treatment decisions in patient with lung cancer. Although ^{18}F-fluorodeoxyglucose positron emission tomography/computed tomography (^{18}F-FDG PET/CT) has a higher diagnostic accuracy in LN characterization than anatomical imaging, differentiating between metastatic and inflammatory LNs is still challenging because both could show high ^{18}F-FDG uptake. The purpose of this study was to assess if the heterogeneity of the ^{18}F-FDG uptake could help in differentiating between inflammatory and metastatic LNs in lung cancer, and to compare with other parameters.
Methods A total of 44 patients with adenocarcinoma of the lung, who underwent preoperative ^{18}F-FDG PET/CT without having any previous treatments and were revealed to have ^{18}F-FDG-avid LNs, were enrolled. There were 52 pathology-proven metastatic lymph nodes in 26 subjects. The pathology-proven metastatic LNs were compared with 42 pathology-proven inflammatory/benign LNs in 18 subjects. The coefficient of variation (CV) was used to assess the heterogeneity of ^{18}F-FDG uptake by dividing the standard deviation of standardized uptake value (SUV) by mean SUV. The volume of interest was manually drawn based on the combined CT images of ^{18}F-FDG PET/CT (no threshold is used). Comparisons were made with the maximum standardized uptake values (SUVmax), visual assessment of ^{18}F-FDG uptake, longest diameter, and maximum Hounsfield units (HUmax).
Results Metastatic lymph nodes tended to have higher CVs than the inflammatory LNs. The mean CV of metastatic LNs (0.30±0.08; range: 0.08–0.55) was higher than that of inflammatory LNs (0.17+0.06; range, 0.07–0.32; $P<0.0001$). On receiver operating characteristic (ROC) curve analysis, the area under curve was 0.901, and using 0.20 as cut-off value, sensitivity, specificity, positive predictive value (PPV), negative predictive value (NPV), and accuracy were 88.5 %, 76.2 %, 82.2 %, 84.3, and 83.0 % respectively. Accuracy of CV was slightly higher than SUVmax and diameter, but significantly higher than visual assessment and HUmax.
Conclusions In patients with adenocarcinoma of the lung having no prior treatments, metastatic LNs showed more heterogeneous ^{18}F-FDG uptake than inflammatory LNs. Measuring the CV of the SUV derived from a manual volume of interest (VOI) can be helpful in determining metastatic LN of adenocarcinoma of the lung. Including diagnostic criteria of CV into the diagnostic approach can increase the accuracy of mediastinal node status.

Keywords Heterogeneity · ^{18}F-FDG uptake · Positron emission tomography (PET) · Lymph node metastasis · Adenocarcinoma of the lung

H. Budiawan · G. J. Cheon · H.-J. Im · S. J. Lee · J. C. Paeng · K. W. Kang · J.-K. Chung · D. S. Lee
Department of Nuclear Medicine, Seoul National University Hospital, Seoul, Korea

H. Budiawan
Department of Nuclear Medicine, Mochtar Riady Comprehensive Cancer Centre, Siloam Hospitals Semanggi, Jakarta, Indonesia

G. J. Cheon · K. W. Kang
Cancer Research Institute, Seoul National University, Seoul, Korea

G. J. Cheon (✉)
Department of Nuclear Medicine, Seoul National University College of Medicine, 101 Daehangro, Jongro-gu, Seoul 110-744, Korea
e-mail: larrycheon@gmail.com

Introduction

Lymph node (LN) characterization is crucial in the diagnosis of lung cancer. The spreading of cancer to LNs determines the stage, treatment decisions, and prognosis. Mediastinal lymphadenopathy may be caused by either inflammatory or malignant diseases. Anatomical imaging, such as computed tomography (CT) scan, is not too accurate, in that 28 % of enlarged LNs on CT were proven to be negative and 20 % of non-enlarged mediastinal LNs were positive of metastasis on histopathology [1, 2].

Although ^{18}F-fluorodeoxyglucose positron emission tomography/computed tomography (^{18}F-FDG PET/CT) had a higher diagnostic accuracy in LN characterization than anatomical imaging in prospective study [3, 4], differentiating between metastatic and inflammatory LNs is still challenging because both kinds of LN status can show high ^{18}F-FDG uptake on PET. Furthermore ^{18}F-FDG PET-CT had low positive predictive value (PPV) in LN staging in patients with operable non-small-cell lung cancer [2, 5].

Malignancy is known to have increased aerobic glycolysis [6], which becomes the biologic basis in ^{18}F-FDG PET imaging. ^{18}F-FDG PET is known to be relatively sensitive in detecting malignancy. However, inflammation can be a potential cause of false-positive findings mimicking malignancy as Glut-1 expression is also higher, and thus glucose metabolism is elevated in inflammatory lesion [7]. Inflammatory cells like activated granulocytes, lymphocytes, and macrophages are well known to have increased glycolysis due to the high amount of glucose transporters [8–10].

Tissue heterogeneity is an important factor contributing to the total FDG uptake in tumors as stated by Avril et al. [11]. In a breast cancer study, they showed that the relative composition of malignant tumors ranged from a few transformed cells to 90 % malignant cells. In a human adenocarcinoma cell line in vitro, Higashi et al. [12] also showed that ^{18}F-FDG uptake also depended on the number of viable cancer cells. The non-malignant component of tumors, however, also contributed to the overall uptake of ^{18}F-FDG. Kubota et al. [9] showed that besides in tumor cells, ^{18}F-FDG accumulation was also found in inflammatory components related to the growth or necrosis of a tumor. Brown et al. [10] showed that non-malignant components were also observed with low metabolic activity such as in granulation tissue, inflammatory infiltration, connective tissue stroma, and necrotic areas. Therefore, it is reasonable to be considered that ^{18}F-FDG uptake from malignant tumors can have more heterogeneity in distribution.

The purpose of this study was to assess if heterogeneity of ^{18}F-FDG uptake can help in differentiating between metastatic and inflammatory lymphadenopathy in lung adenocarcinoma in comparison with other parameters of ^{18}F-FDG PET and CT.

Materials and Methods

Study Population

All subjects of this retrospective study underwent initial ^{18}F-FDG PET/CT work-up (without any prior treatment) during 2011 and turned out to have ^{18}F-FDG-avid LNs and underwent further pathologic studies. In order to have a homogeneous data set, subjects of this study were limited to the patients with adenocarcinoma of the lung, which was known to have varied ^{18}F-FDG uptake and thus often resulting in false-negative findings. The biopsy-proven metastatic LNs were compared with biopsy-proven benign/inflammatory hypermetabolic LNs. Most nodal station biopsies were guided by PET/CT findings. The histopathologic diagnoses of all mediastinal, hilar, and interlobar LNs were obtained by surgical resection, endobronchial ultrasound biopsy, or gun biopsy, while supraclavicular and cervical LNs were obtained by excision or needle biopsy.

Lymph Node Station

All ^{18}F-FDG-avid LNs proven by biopsy as metastatic adenocarcinoma from lung or benign within 4 weeks after ^{18}F-FDG PET imaging were included. The exclusion criterion was longest diameter less than 5 mm. LN stations were assigned according to the Association for the Study of Lung Cancer.

^{18}F-FDG PET protocol

After fasting for at least 6 h, approximately 5.18 MBq/kg (0.14 mCi/kg) of ^{18}F-FDG was intravenously administered. Blood glucose level should be less than 11.0 mmol/l (200 mg/dl). Imaging acquisitions were performed approximately 60 min after ^{18}F-FDG injection using Biograph PET/CT scanners (Siemens medical solution, TN, USA). CT scans were performed for attenuation correction and anatomical correlation (120 kVp, 40 mAs, pitches of 1.2). PET acquisitions were performed with 1 min per bed position from skull base to proximal thigh. PET reconstructions were done using a point spread function-based iterative algorithm (TrueX, 2 iterations, 21 subsets) with matrix size of 256×256.

Image Analysis

After image reconstruction, the volume of interest (VOI) of the LNs was determined by making region of interest (ROI) in every image slice of the LNs on the combined CT images of ^{18}F-FDG PET/CT using freeform method in the Syngo Oncology Engine with TrueD workstation (Siemens, Erlangen, Germany). No threshold was used. If there were many/conglomerated LNs in the area in which pathologic studies were done, VOI delineations were performed to the highest

SUVmax with the most well-defined lesions. Careful delineation was done to make sure that no background or adjacent LN area was included.

From the VOI made, all necessary data were obtained, including SUVmax, mean of SUV (SUVmean), standard deviation of SUV, longest diameter, and maximum Hounsfield units (HUmax). Uptake of the ^{18}F-FDG-avid LNs was also visually scored using three grades of intensity of mediastinal blood pool (0=similar with mediastinal blood pool, 1=faintly positive, 2=definitely positive). SUV threshold of 2.5 was used for differentiating between metastatic and benign LNs in lung cancer [13–15]. Highly attenuated nodes were defined as those that had HU max >120 [16] as one of the diagnostic criteria in determining benign LN in patients with non-small-cell lung cancer.

Heterogeneity of ^{18}F-FDG Uptake

The coefficient of variation (CV) was used to assess the heterogeneity of ^{18}F-FDG uptake by dividing the standard deviation of the SUV by the SUVmean. The VOI was made based on the manually drawn ROI on every image slice (no threshold was used) in order to include all ^{18}F-FDG uptake in the tumor volume, even areas with very low/no uptake such as necrotic area. In case of automatic VOI, there was a potency to lose area with ^{18}F-FDG uptake below the selected threshold, which might result in improper values. To reduce the incorrect value of the heterogeneity, we used the manually drawn ROI method in this study.

Statistical Analysis

Independent sample *t*-tests were used to compare the means of CV, SUVmax, diameter, volume, and HUmax in the metastatic and benign LNs groups. The performance of these parameters in differentiating metastatic from benign LNs was analyzed using the receiver operating characteristic (ROC) curve. Univariate and multivariate logistic regression analysis were used to explore the role of the existing variables in predicting metastatic LNs. Statistical analysis was performed using MedCalc version 12.5.0 (MedCalc, Ostend, Belgium).

Results

Patients' Characteristics

A total of 44 subjects suffering from adenocarcinoma of the lung who underwent initial ^{18}F-FDG PET/CT work-up (without any prior treatment) were included in this study. All subjects had FDG-avid LNs in interlobar, hilar, mediastinal, supraclavicular, and/or cervical stations. Metastatic LNs were found in 26 subjects (15 men and 11 women; mean age, 63.3±9.9 years; range 42–76); while inflammatory LNs were found in 18 subjects (10 men and 8 women; mean age 68.1±7.7 years; range 52–85). All the primary lung lesions were pathology-proven as primary adenocarcinoma of the lung. All LNs were also proven as malignant/metastatic or benign/inflammatory/having no malignancy. Analysis was done to 52 metastatic LN stations compared with 42 benign LN stations (Table 1).

All subjects with metastatic LNs were reported to have just adenocarcinoma (n=24, five of them as poorly differentiated adenocarcinoma) and two with invasive adenocarcinoma: mixed solid and bronchioloalveolar pattern (n=1) and mixed acinar and papillary pattern (n=1). Fourteen of them (53.8 %) had N3 disease (metastasis in contralateral mediastinal, contralateral hilar, supraclavicular, or cervical), 11 (42.3 %) had N2 disease, and one (3.8 %) had N1 disease. Distant metastasis was observed in 20 subjects in bone, lung, liver, adrenal, pleura, pericardiac, and soft tissue.

Patients without metastatic LNs were reported to have just adenocarcinoma (n=2), 14 with invasive adenocarcinoma: acinar pattern (n=3), mixed acinar and bronchioloalveolar pattern (n=6), predominantly solid pattern (n=1), mucinous and non-mucinous (acinar) type (n=1), mixed acinar and micropapillary pattern (n=3), and two with preinvasive lesions: adenocarcinoma in situ (n=1) and mixed mucinous/non-mucinous bronchioloalveolar (n=1). N status was considered as N0 in all subjects in this group. Distant metastasis was only found in one patient (bone metastasis). N staging and distant metastasis were assumed based on ^{18}F-FDG PET and pathologic findings (Table 2).

Diagnostic Performance of Visual Assessment

By visual assessment of ^{18}F-FDG PET, 56 LNs (59.6 %) were definitely positive, 32 (34.0 %) were faintly positive, and 6 (6.4 %) were negative. In the malignant LNs, 42 (80.8 %)

Table 1 Distribution of Metastatic and Inflammatory LNs

Location	Metastatic LNs	Benign LNs
4 (lower jugular/cervical)	3	–
1 (supraclavicular)	7	–
2 (upper paratracheal)	6	–
4 (lower paratracheal)	15	9
5 (subaortic)	–	5
6 (para-aortic)	3	1
7 (subcarinal)	10	6
8 (para-oesophageal)		1
10 (hilar)	3	13
11 (interlobar)	5	6
12 (lobar)	–	1
Total	52	42

Table 2 Patients' Characteristics

	Metastatic LNs (26 patients, 52 LNs)	Benign LNs (18 patients, 42 LNs)
Age (years)	63.3±9.9	68.1±7.7
Sex		
male	15	10
female	11	8
N staging		
N0	–	18 (100%)
N1	1 (3.8%)	–
N2	11 (42.3%)	–
N3	14 (53.8%)	–
Distant metastases	20 (76.9%)	1 (5.6%)
Pathologic findings of primary lung cancer		
adenocarcinoma[a]	24	2
invasive adenocarcinoma	2	14
preinvasive lesions	–	2
Pathologic finding of LNs	Metastatic adenocarcinoma	No metastases

N staging was assumed based on FDG PET scan and pathologic finding

[a] Described as just adenocarcinoma

were definitely positive, 8 were faintly positive (15.4 %), and 2 (3.8 %) were negative. While in the benign LNs, 14 (33.3 %) were definitely positive, 24 (57.1 %) were faintly positive, and 4 (9.5 %) were negative (Table 3). ROC curve analysis using the visual assessment data for the determining malignancy with cutoff value >1 revealed the sensitivity, specificity, PPV, negative predictive value (NPV), and accuracy of 80.8 %, 66.7 %, 75.0 %, 73.7 %, and 74.5 %, respectively (area under curve [AUC] 0.734, Fig. 1a).

Diagnostic Performance of SUVmax

SUVmax was significantly higher in metastatic LNs (9.79±4.51; range 1.98–21.79) than benign LNs (4.96±2.08; range 2.20–11.22; $P<0.0001$). Using SUVmax of 2.5 as cutoff value as the common value used, there were 51 true-positives (TPs) results, 2 true-negatives (TNs), 40 false-positives (FPs), and 1 false-negative (FN) (Table 3) yielding sensitivity, specificity, PPV, NPV, and accuracy of 98.1 %, 4.8 %, 56.0 %, 66.7 %, and 57.0 % respectively. ROC analysis of this study revealed the optimal cutoff of >5.96 with sensitivity, specificity, PPV, NPV, and accuracy of 84.6 %, 76.2 %, 81.5 %, 80.0 %, and 80.9 % respectively (AUC 0.857, Fig. 1b).

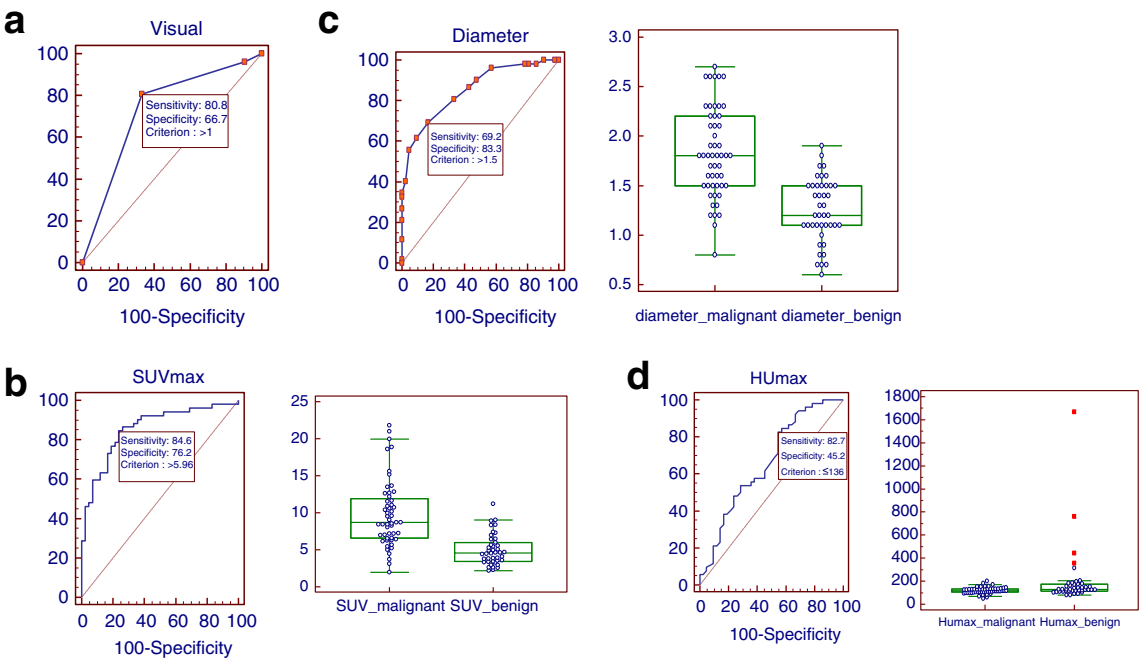

Fig. 1 Receiver operating characteristic (ROC) analysis of visual assessment, SUVmax, longest diameter, and HUmax in determining malignancy. **a** Visual assessment with cutoff value >1 revealed sensitivity, specificity, PPV, NPV, and accuracy of 80.8 %, 66.7 %, 75.0 %, 73.7 %, and 74.5 % respectively (AUC 0.734). **b** SUVmax analysis revealed the optimal cutoff of >5.96 with sensitivity, specificity, PPV, NPV, and accuracy of 84.6 %, 76.2 %, 81.5 %, 80.0 %, and 80.9 % respectively (AUC 0.857). Comparison graphs showed the distribution of SUVmax in malignant and benign LNs (*right*). **c** Longest diameter analysis revealed the optimal cutoff of >1.5 cm with sensitivity, specificity, PPV, NPV, and accuracy of 69.2 %, 83.3 %, 83.7 %, 68.6 %, and 75.5 % respectively (AUC 0.851). Comparison graphs showed the distribution of longest diameter in malignant and benign LNs (*right*). **d** HUmax analysis revealed the optimal cutoff of ≤136 with sensitivity, specificity, PPV, NPV, and accuracy of 82.7 %, 45.2 %, 65.1 %, 67.8 %, and 66.0 % respectively (AUC 0.661). Comparison graphs showed the distribution of HUmax in malignant and benign LNs (*right*)

Table 3 Comparison of CV and Other Parameters (Visual Assessment, SUVmax, Longest Diameter, HUmax) Using the Known Cutoff in Determining Metastatic LNs

		Pathologic finding		
		Metastasis	Benign	Total
^{18}F-FDG PET—visual analysis	Definitely positive	42 (80.8 %)	14 (33.3 %)	56 (59.6 %)
	Faintly positive	8 (15.4 %)	24 (57.1 %)	32 (34.0 %)
	Negative	2 (3.8 %)	4 (9.5 %)	6 (6.4 %)
	Total	52	42	94
^{18}F-FDG PET parameter—SUVmax[a]	≥2.5	51 TP	40 FP	91
	<2.5	1 FN	2 TN	3
	Total	52	42	94
CT parameter—longest diameter[a]	>10 mm	51 TP	34 FP	85
	≤10 mm	1 FN	8 TN	9
	Total	52	42	94
CT parameter—HU[a]	≤120	28 TP	13 FP	41
	>120	24 FN	29 TN	53
	Total	52	42	94
^{18}F-FDG PET parameter—CV[a]	>0.2	46 TP	10 FP	56
	≤2.0	6 FN	32 TN	38
	Total	52	42	94

TP true positive, *FP* false positive, *TN* true negative, *FN* false negative

[a] SUVmax of ≥2.5, diameter of >1.0 cm, HUmax ≤120, CV >0.20 were used as cutoff value

Diagnostic Performance of Longest Diameter of LNs

Diameter of LN is well known to have relation with the probability of malignancy. The mean diameter of metastatic LNs (1.83±0.45, range 0.8–2.7 cm) was significantly longer than benign LNs (1.25±0.32, range 0.6–1.9; $P<0.0001$). The common value of the diameter used in determining malignant LNs is >1.0 cm. Using that criterion, there were 51 TPs, 8 TNs, 34 FPs, and 1 FN result (Table 3), yielding sensitivity, specificity, PPV, NPV, and accuracy of 98.1 %, 19.1 %, 60.0 %, 88.9 %, and 62.8 % respectively. The ROC analysis of this study revealed an optimal cutoff of >1.5 cm for sensitivity, specificity, PPV, NPV, and accuracy of 69.2 %, 83.3 %, 83.7 %, 68.6 %, and 75.5 % respectively (AUC 0.851, Fig. 1c).

Diagnostic Performance of HUmax

The mean value of HUmax in metastatic LNs was 119.0±27.9 (range 48–202) which was also significantly lower than benign LNs (201.5±259.6, range 78–1,667; $P=0.0249$). Using HUmax ≤120 as cutoff value, there were 28 TPs, 29 TNs, 13 FPs, and 24 FN results (Table 3) yielding sensitivity, specificity, PPV, NPV, and accuracy of 53.9 %, 69.1 %, 68.3 %, 54.7 %, and 60.6 % respectively. From ROC analysis of this study, it was found out that the optimum cutoff value was ≤136 with sensitivity, specificity, PPV, NPV, and accuracy of 82.7 %, 45.2 %, 65.1 %, 67.8 %, and 66.0 % respectively (AUC 0.661, Fig. 1d).

Heterogeneity of LN on FDG PET

Metastatic LNs tend to have a higher CV compared with inflammatory LNs ($P<0.0001$). The mean CV of metastatic LNs was 0.30±0.08 (range 0.08–0.55), while inflammatory LNs was 0.17±0.06 (range 0.07–0.32). On ROC analysis, the AUC was 0.901, and the cutoff value was >0.20 with 46 TPs, 32 TNs, 10 FPs, and 6 FNs results yielding sensitivity, specificity, PPV, NPV, and accuracy of 88.5 %, 76.2 %, 82.2 %, 84.3 %, and 83.0 % respectively (Table 3 and Fig 2).

Comparison Between CV and Other Methods

Compared with other parameters described above, CV has the highest AUC and accuracy, which were slightly higher than SUVmax and diameter, but significantly

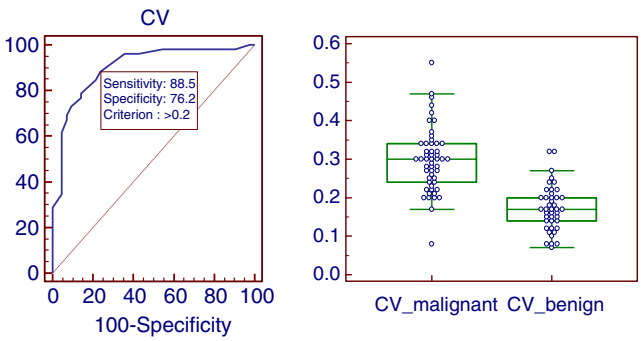

Fig. 2 ROC analysis of the CV revealed an optimal cutoff of >0.20 with sensitivity, specificity, PPV, NPV, and accuracy of 88.5 %, 76.2 %, 82.2 %, 84.3 %, and 83.0 % respectively. Comparison graphs showing the distribution of CVs in malignant and benign LNs (*right*)

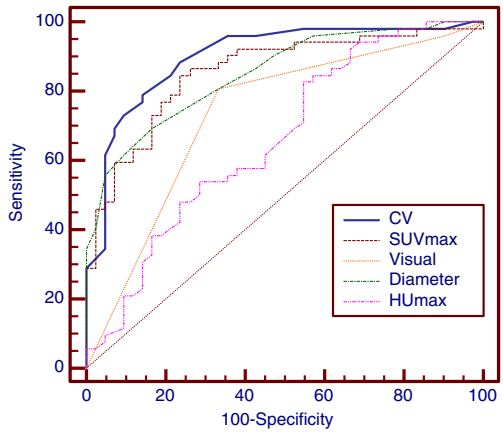

Fig. 3 Comparison between CV and other parameters. CV had the highest AUC of 0.901 which was slightly higher than diameter and SUVmax, but significantly higher than visual assessment and HUmax

higher than visual assessment and HUmax (Fig 3). CV had the highest sensitivity followed by SUVmax, HUmax, and visual assessment, while diameter had the lowest sensitivity but highest specificity, which was slightly better than CV and SUVmax. Diameter, CV, and SUVmax did not have any significant difference in PPV. CV and SUVmax were also superior in NPV than other parameters (Table 4).

Univariate logistic regression showed that all parameters were significant predictors, except visual assessment. In multivariate logistic regression (with four predictors: SUVmax, diameter, HUmax, and CV), CV and diameter were statistically significant. SUVmax was not regarded as a significant predictor and HUmax had only borderline significance (Tables 5 and 6).

Diagnostic Strategy in Determining LN Metastasis

The first step proposed is determining SUVmax, since it is more sensitive than other parameters (except CV) and SUVmax measurement is very simple. No benign LNs had SUVmax >11.22, meaning LNs with SUVmax above this level were malignant and did not need analysis of other parameters. This level (>11.22) and >5.96 as SUVmax cutoff value divided the LNs into three subgroups (Fig. 4).

If SUVmax is >5.96 but ≤11.22, then CV can be used for the further analysis. Metastasis is more likely if the CV is >0.20; but if the CV is ≤0.20, then the value of the longest diameter should be considered. If the diameter is >1.5 cm, then metastasis is suggested; otherwise (diameter ≤1.5 cm), a benign process is suspected. In Fig. 5a, a hypermetabolic subcarinal LN of a 50-year-old man was observed with SUVmax of 9.57. The CV was 0.31, indicating a metastatic process (diameter=1.8 cm, but HUmax=202). In Fig. 5b, hypermetabolic cervical LN in 49-year-old woman with lung adenocarcinoma of the left upper lobe showed an SUVmax of 8.05 with a CV of 0.42, indicating metastatic process. HUmax was 48, also suggesting metastatic process, as confirmed by pathologic finding, although the longest diameter was only 0.8 cm. In Fig. 5c, intense FDG-avid left hilar LN in 85-year-old man showed an SUVmax of 8.94, but negative finding from the CV, diameter, and HUmax (0.12, 1.2 cm, and 169 respectively), suggesting a benign lesion, compatible with the pathologic finding.

If SUVmax is ≤5.96, the CV value should also be considered. If the CV is ≤0.20, a benign process is suspected. If the CV is >0.20, then measurement of the LN diameter will be helpful. A diameter of >1.5 cm indicates metastasis; otherwise (≤1.5 cm) a benign process is more likely. In Fig. 6a, a 76-year-old man with adenocarcinoma of the right upper lobe of the lung showed an ^{18}F-FDG-avid right lower paratracheal LN with SUVmax of 5.43 (under cutoff value), but the CV was 0.30, with a diameter of 1.6 cm (HUmax was 113), indicating a metastatic process. Pathologic finding confirmed it as metastatic adenocarcinoma. In Fig. 6b, ^{18}F-FDG-avid right interlobar and hilar LNs adjacent to the adenocarcinoma lung lesion were observed with SUVmax of 5.06 and 3.27. CV values were below 0.20 (0.15 and 0.15), indicating a benign process. The diameters of both LNs also indicated a benign process (1.5 and 1.5 cm), and the HUmax values were 115 and 142, respectively. Using this strategic approach, the

Table 4 Statistical comparisons among CT and FDG PET parameters

	Visual assessment	SUVmax	Diameter	HUmax	CV
Mean value of metastatic LNs	–	9.79±4.51 (1.98–21.79)	1.83±0.45 (0.8–2.7)	119.0±27.9 (48–202)	0.30+0.08 (0.08–0.55)
Mean value of benign LNs	–	4.96±2.08 (2.2–11.22)	1.25±0.32 (0.6–1.9)	201.5±259.6 (78–1667)	0.17±0.06 (0.07–0.32)
AUC	0.734	0.857	0.851	0.661	0.901
Sensitivity (%)	80.8	84.6	69.2	82.7	88.5
Specificity (%)	66.7	76.2	83.3	45.2	76.2
PPV (%)	75.0	81.5	83.7	65.1	82.2
NPV(%)	73.7	80.0	68.6	67.8	84.3
Accuracy (%)	74.5	80.9	75.5	66.0	83.0

AUC area under curve, *PPV* positive predictive value, *NPV* negative predictive value

Table 5 Univariate Logistic Regression of CT and FDG PET Parameters

	Univariate			
Predictor	Coefficient	OR	95 % CI	*P*
Visual assessment				
grade1	−0.41	0.67	0.10–4.35	0.6719
grade2	1.79	6.00	0.99–36.37	0.0513
SUVmax	0.54	1.71	1.36–2.16	<0.0001
Diameter	4.05	57.40	10.19–323.25	<0.0001
HUmax	−0.02	0.98	0.97–0.10	0.0143
CV	26.76604	4.21E+11	1.01E+7 to 17.5E+015	<0.0001

OR odds ratio, *CI* confidence interval, *AUC* area under curve

sensitivity, specificity, PPV, NPV, and accuracy were 92.3 %, 83.3 %, 87.3 %, 89.7 %, and 88.3 % respectively.

Discussion

Inflammation has a critical role in tumorigenesis [17], from initiation, promotion, malignant conversion, invasion, and metastatic progression [18]. Inflammatory conditions can be present either before or after a malignant change occurs. In the microenvironment of most malignancies, inflammatory cells and mediators (chemokines, cytokines, and prostaglandins) are observed. Various oncogenes coordinate inflammatory transcriptional programs linking to angiogenesis [19]. Karin [17] stated that inflammation promoted neoangiogenesis and provided surviving cancer cells with additional growth factors produced by the inflammatory and immune cells. Angiogenesis is definitely an important factor in the metastatic process, because in order to survive, grow, and multiply at the site of metastasis, the tumor cells must induce angiogenesis [20, 21].

Angiogenesis is initially induced by certain oncogenes, such as RAS and MYC family members, which recruit leukocytes, expression of tumor-promoting chemokines, and cytokines leading to remodeling of the tumoral microenvironment and finally angiogenesis [22, 23]. While angiogenic activity in tumors seems to be heterogeneous, the extent and density of the angiogenesis were reported to be correlated with the degree of tumor grade [24]. ^{18}F-FDG has been considered to be taken up by angiogenesis process as measured by immunohistochemistry bioassay using CD105, a marker of neovascularization [25, 26]. At some point, the growth of solid malignancies exceeds blood supply, causing oxygen and nutrient shortage, forming a necrotic portion [27]. Necrosis is considered to have very low ^{18}F-FDG uptake and will increase the heterogeneity.

From the above description, it can be assumed that distribution of ^{18}F-FDG uptake in metastatic LNs is affected by several components, namely viable metastatic cells, inflammatory infiltrates, granulation tissue, microvessels/angiogenesis, connective tissue stroma, and necrotic areas. Each of them has its own level of ^{18}F-FDG uptake, resulting in more heterogeneous ^{18}F-FDG uptake represented in CV of SUV. The wide range of CV values of metastatic LNs in this study (from 0.08 to 0.55) might be due to difference of the metastatic phase in the LNs. Different metastatic phases may also have different grades of inflammation, angiogenesis, and necrosis which overall will influence the degree of heterogeneity of FDG uptake.

^{18}F-FDG uptake in benign LN has been correlated with glucose transporter 1 (Glut-1) expression in follicular centre cells. The level of hyperplasia in these follicular centers was more intense, with more Glut-1 expression than non-^{18}F-FDG-avid LNs [7, 28]. Takamochi et al. [29] also found that all LNs with ^{18}F-FDG uptake due to inflammatory conditions showed reactive lymphoid hyperplasia histologically, which was described as reversible benign enlargement caused by antigen stimulation. After being stimulated, follicle multiplication and enlargement, as well as sinus enlargement filled by histiocytes were observed. Lymphocytes, immunoblasts, and macrophages would also be found. There are four known patterns of reactive lymphoid hyperplasia: follicular, diffuse, sinus, and mixed pattern with idiopathic follicular pattern is the most common finding [30]. With predominant diffuse inflammatory infiltrate as the major component taking up ^{18}F-FDG, it is assumable that the heterogeneity of ^{18}F-FDG uptake in the inflammatory LNs in this study was less heterogeneous than metastatic ones. The considerable range of CVs for inflammatory LNs (0.07–0.32) in this study might be due

Table 6 Multivariate Logistic Regression of CT and FDG PET Parameters

	Multivariate			
Predictor	Coefficient	OR	95 % CI	*P*
SUVmax	0.24	1.27	0.90–1.79	0.182
Diameter	3.99	54.25	4.18–703.83	0.0023
HUmax	−0.02	0.98	0.95–1.00	0.0489
CV	14.84	2.79E+06	3.5818 to 2.17E+012	0.032

OR odds ratio, *CI* confidence interval, *AUC* area under curve

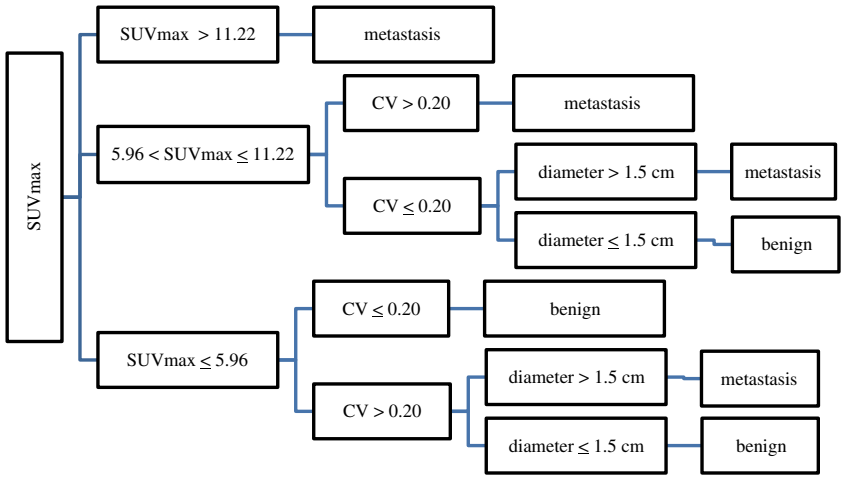

Fig. 4 Diagnostic strategy in determining LN metastasis

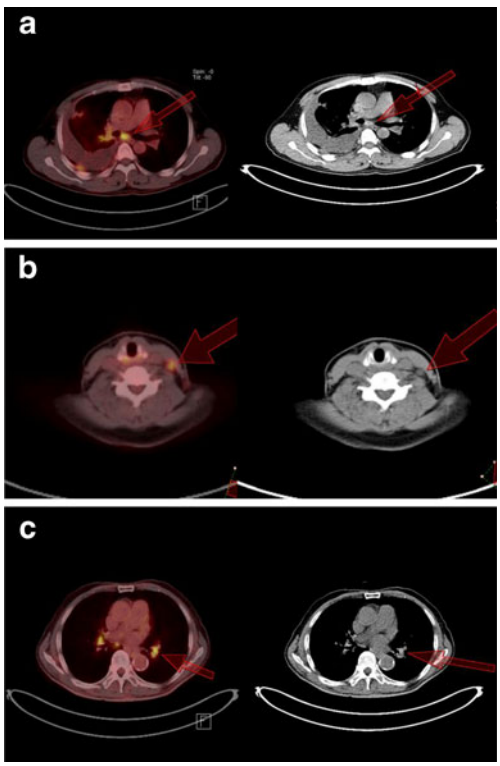

Fig. 5 If the SUVmax is >5.96 but ≤11.22, the CV could be used for the further analysis. If the CV is >0.20, then metastasis is more likely; but if the CV is ≤0.20, then the value of the longest diameter should be determined. A diameter of >1.5 cm suggests metastasis, otherwise (diameter ≤1.5 cm) a benign process is more likely. **a** A 50-year-old man with adenocarcinoma of the right lobe of the lung showed hypermetabolic subcarinal LN with SUVmax, CV, and longest diameter of 9.57, 0.31, and 1.8 cm, respectively, indicating metastatic process in keeping with pathologic finding, despite of high HUmax of 202. **b** Hypermetabolic cervical LN in a 49-year-old woman with lung adenocarcinoma of the left upper lobe showed SUVmax of 8.05. The CV was 0.42, indicating metastasis, as confirmed by pathologic finding. HUmax of 48 also suggested metastatic process, although longest diameter was only 0.8 cm. **c** Intense FDG-avid left hilar LN in an 85-year-old man showed an SUVmax of 8.94, but a negative finding from CV, diameter, HUmax (0.12, 1.2 cm, and 169 respectively) suggested a benign lesion compatible with the pathologic finding. The primary adenocarcinoma was in the left upper lobe of lung

to the different patterns, which in turn caused different heterogeneity of ^{18}F-FDG uptake.

Several studies have used an SUV threshold of 2.5 for differentiating benign and metastatic mediastinal LN in lung cancer [13–15]. Hellwig et al. [13] preferred to use 2.5 as cutoff value, instead of 4.5 as their best accuracy, in order to reduce the FN results. In our study the cutoff value for SUVmax determined from the ROC curve was 5.96, which

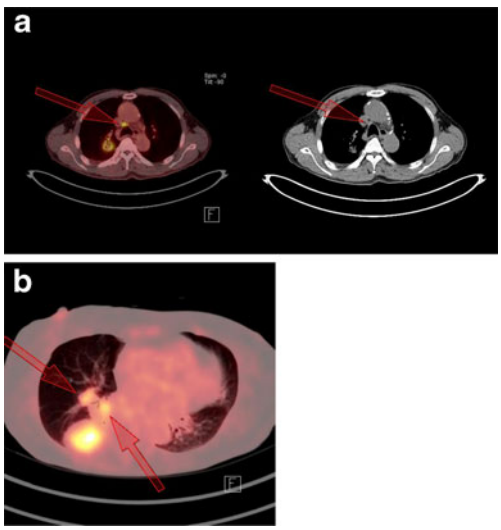

Fig. 6 If the SUVmax is ≤5.96, the CV value should also be considered. If the CV is ≤0.20, a benign process is suspected. If the CV is >0.20, then measurement of the diameter will be helpful. A diameter >1.5 cm indicats metastasis; otherwise (≤1.5 cm) a benign process is more likely. **a** FDG-avid right lower paratracheal LN was observed with an SUVmax of 5.43 (under the cutoff value), but CV was 0.30 with a diameter of 1.6 cm (HUmax was 113) indicating metastatic process. Pathologic finding confirmed as metastatic adenocarcinoma. This 76-year-old man had primary adenocarcinoma of right upper lobe of lung. **b** FDG-avid right interlobar and hilar LNs adjacent to the adenocarcinoma lung lesion were observed with SUVmax of 5.06 and 3.27. CV values were below 0.20 (0.15 and 0.15) indicating benign process in keeping with pathologic findings. Diameter of both LNs also indicated benign process (1.5 and 1.5 cm). HUmax values were 115 and 142

was still in the range of the finding from other studies varying from 4.2 to 6.2 [31–34], although our study only focused on adenocarcinoma of the lung subjects. The accuracy of CV and SUVmax were similar (83.0 vs 80.9), but the correlation between them was only moderate (R^2 0.4237; calculation is not shown), meaning there were cases of pathology-proven metastatic LNs having a negative finding of SUVmax but positive finding of CV, and also benign LNs having a positive finding of SUV but with a negative finding of CV.

Clinical applicability of CT in assessing LN is limited. Enlarged nodes may be not malignant and non-enlarged nodes may be malignant [35]. From many CT studies, the ranges of sensitivity and specificity in detecting mediastinal LN metastasis were between 51 % (47–54 %) and 85 % (84–88 %) respectively [36]. In our study, the sensitivity was higher (69.2 %) with similar specificity (83.3 %). Probably the cause is the different criterion used. The accepted criterion of normal-sized mediastinal LNs in CT is ≤1.0 cm measured in short-axis [36], while the longest diameter of LNs in our study was measured based on VOI and could be in any axis.

In CT, attenuation which was higher than the surrounding great vessels was known to indicate benign lymphadenopathy. The common histopathologic findings were cortical follicular hyperplasia with anthracotic pigmentation and macrophage infiltration. Microscopic fibrotic nodules could also be found in the medulla [37, 38]. A similar study also showed that calcification or high attenuation at LNs on CT, even with ^{18}F-FDG activity, indicated they were benign in a tuberculosis endemic region [39]. Our study showed that HUmax analysis was less accurate than other parameters in differentiating metastatic from inflammatory LNs.

The accuracy of CVs derived from manual VOIs in differentiating metastatic and inflammatory LNs was slightly better than SUVmax. Overall the accuracy of ^{18}F-FDG parameters (CV 83.0 %; SUVmax 80.9 %,) were higher than CT parameters (diameter 75.5 %; HUmax 66.0 %). A limitation of our study was that low-dose unenhanced CT was used as the CT part of the ^{18}F-FDG PET/CT scan.

Conclusions

In adenocarcinoma of the lung in subjects having no prior treatments, metastatic LNs showed more heterogeneous ^{18}F-FDG uptake than inflammatory LNs. Measuring the CV of the SUV derived from a manual VOI can be helpful in determining metastatic LN of adenocarcinoma of the lung. Including CV into the diagnostic approach will increase the accuracy.

Conflicts of interest None.

References

1. Pieterman RM, Van Putten JW, Meuzelaar JJ, Mooyaart EL, Vaalburg W, Koeter GH, et al. Preoperative staging of non-small cell lung cancer with positron-emission tomography. N Eng J Med. 2000;343:254–61.
2. De Leyn P, Vansteenkiste J, Cuypers P, Deneffe G, Van Raemdonck D, Coosemans W, et al. Role of cervical mediastinoscopyin staging of non-small cell lung cancer without enlarged mediastinal lymph nodes on CT scan. Eur J Cardiothorac Surg. 1997;12:706–12.
3. Fischer B, Lassen U, Morten J, Larsen S, Loft A, Bertelsen A, et al. Preoperative staging of lung cancer with combined PET-CT. N Eng J Med. 2009;361:32–9.
4. Perigaud C, Bridji B, Roussel JC, Sagan C, Mugniot A, Duveau D, et al. Prospective preoperative mediastinal lymph node staging by integrated positron emission tomography-computerised tomography in patients with non-small-cell lung cancer. Eur J Cardiothorac Surg. 2009;36:731–6.
5. Yang W, Fu Z, Yu J, Yuan S, Zhang B, Li D, et al. Value of PET/CT versus enhanced CT for locoregional lymph nodes in non-small cell lung cancer. Lung Cancer. 2008;61(1):35–43.
6. Warburg O, Wind F, Negelein E. The metabolism of tumors in the body. J Gen Physiol. 1927;8:519–30.
7. Chung JH, Cho KJ, Lee SS, Baek HJ, Park JH, Cheon GJ, et al. Overexpression of Glut1 in lymphoid follicles correlates with false-positive ^{18}F-FDG PET results in lung cancer staging. J Nucl Med. 2004;45:999–1003.
8. Kubota R, Kubota K, Yamada S, Tada M, Ido T, Tamahashi N. Active and passive mechanisms of [fluorine-18]fluorodeoxyglucose uptake by proliferating and prenecrotic cancer cells in vivo: A microautoradiographic study. J Nucl Med. 1994;35:1067–75.
9. Kubota R, Yamada S, Kubota K, Ishiwata K, Tamahashi N, Ido T. Intratumoral distribution of fluorine-18-fluorodeoxyglucosein vivo: High accumulation in macrophages and granulation tissues studied by microautoradiography. J Nucl Med. 1992;33:1972–80.
10. Brown RS, Leung JY, Fisher SJ, Frey KA, Ethier SP, Whal RL. Intratumoral distribution of tritiatedfluorodeoxyglucose in breast carcinoma. I. Are inflammatory cells important? J Nucl Med. 1995;36:1854–61.
11. Avril N, Menzel M, Dose J, Schelling M, Weber W, Jänicke F, et al. Glucose metabolism of breast cancer assessed by 18F-FDG PET: Histologic and immunohistochemical tissue analysis. J Nucl Med. 2001;42:9–16.
12. Higashi K, Anaira CC, Wahl RL. Does FDG uptake measure proliferative activityof human cancer cells? In vitro comparison with DNA flow cytometry and tritiated thymidine uptake. J Nucl Med. 1993;34:414–9.
13. Hellwig D, Graeter TP, Ukena D, Groeschel A, Sybrecht GW, Schaefers HJ, et al. 18F-FDG PET for mediastinal staging of lung cancer: Which SUV threshold makes sense? J Nucl Med. 2007;48:1761–6.
14. Kernstine KH, Stanford W, Mullan BF, Rossi NP, Thompson BH, Bushnell DL, et al. PET, CT, and MRI with Combidex for mediastinal staging in non-small cell lung carcinoma. Ann Thorac Surg. 1999;68:1022–8.
15. Cerfolio RJ, Bryant AS, Ojha B, Eloubeidi M. Improving the inaccuracies of clinical staging of patients with NSCLC: A prospective trial. Ann Thorac Surg. 2005;80:1207–13.
16. Cho YS, Choi JY, Lee KS, Kwon OJ, Shim YM, Lee SJ, et al. FDG PET/CT criteria for diagnosing mediastinal lymph node metastasis in patients with non-small cell lung cancer. J Nucl Med. 2007;48 (Suppl 2):85P.
17. Karin M. Nuclear factor-kappaB in cancer development and progression. Nature. 2006;441:431–6.
18. Grivennikov SI, Greten FR, Karin M. Immunity, inflammation, and cancer. Cell. 2010;140:883–99.

19. Mantovani A, Allavena P, Sica A, Balkwill F. Cancer-related inflammation. Nature. 2008;454:436–44.
20. Weidner N, Semple JP, Welch WR, Folkman J. Tumor angiogenesis and metastasis: Correlation in invasive breast carcinoma. N Engl J Med. 1991;324:1–8.
21. Hanahan D, Folkman J. Patterns and emerging mechanisms of the angiogenic switch during tumorigenesis. Cell. 1996;86:353–64.
22. Soucek L, Lawlor ER, Soto D, Shchors K, Swigart LB, Evan GI. Mast cells are required for angiogenesis and macroscopic expansion of Myc-induced pancreatic islet tumors. Nat Med. 2007;13:1211–8.
23. Sparmann A, Bar-Sagi D. Ras-induced interleukin-8 expression plays a critical role in tumor growth and angiogenesis. Cancer Cell. 2004;6:447–58.
24. Vamesu S. Angiogenesis and tumor grading in primary breast cancer patients: An analysis of 158 needle core biopsies. Rom J Morphol Embryol. 2006;47:251–7.
25. Groves AM, Shastry M, Rodriguez-Justo M, Malhotra A, Endozo R, Davidson T, et al. ^{18}F-FDG PET and biomarkers for tumour angiogenesis in early breast cancer. Eur J Nucl Med Mol Imaging. 2011;38:46–52.
26. Guo J, Higashi K, Ueda Y, Oguchi M, Takegami T, Toga H, et al. Microvessel density: Correlation with 18F-FDG uptake and prognostic impact in lung adenocarcinomas. J Nucl Med. 2006;47:419–25.
27. Vakkila J, Lotze MT. Inflammation and necrosis promote tumourgrowth. Nat Rev Immunol. 2004;4:641–8.
28. Nguyen XC, So Y, Chung JH, Lee WW, Park SY, Kim SE. High correlations between primary tumours and loco-regional metastatic lymph nodes in non-small-cell lung cancer with respect to glucose transporter type 1-mediated 2-deoxy-2-F18-fluoro-D-glucose uptake. Eur J Cancer. 2008;44:692–8.
29. Takamochi K, Yoshida J, Murakami K, Niho S, Ishii G, Nishimura M, et al. Pitfalls in lymph node staging with positron emission tomography in non-small cell lung cancer patients. Lung Cancer. 2005;47:235–42.
30. Van der Valk P, Meijer CJ. The histology of reactive lymph nodes. Am J Surg Pathol. 1987;11:866–82.
31. Scott WJ, Gobar LS, Terry JD, Dewan NA, Sunderland JJ. Mediastinal lymph node staging of non-small-cell lung cancer: A prospective comparison of computed tomography and positron emission tomography. J Thorac Cardiovasc Surg. 1996;111(3):642–8.
32. Vansteenkiste JF, Stroobants SG, De Leyn PR, Dupont PJ, Bogaert J, Maes A, et al. Lymph node staging in non small-cell lung cancer with FDG-PET scan: a prospective study on 690 lymphnode stations from 68 patients. J Clin Oncol. 1998;16:2142–9.
33. Bryant AS, Cerfolio RJ, Klemm KM, Ojha B. Maximum standard uptake value of mediastinal lymph nodes on integrated FDG-PET-CT predicts pathology in patients with non-small cell lung cancer. Ann Thorac Surg. 2006;82:417–23.
34. Kumar A, Dutta R, Kannan U, Kumar R, Khilnani GC, Gupta SD. Evaluation of mediastinal lymph nodes using ^{18} F-FDG PET-CT scan and its histopathologic correlation. Ann Thorac Med. 2011;6:11–6.
35. Boiselle PM, Patz EF, Vining DJ, Weissleder R, Shepard JA, McLoud TC. Imaging of mediastinal lymph nodes: CT, MR, and FDG PET. Radiographics. 1998;18:1061–9.
36. Silvestri GA, Gould MK, Margolis ML, Tanoue LT, McCrory D, Toloza E, et al. Noninvasive staging of non-small cell lung cancer: ACCP evidenced-based clinical practice guidelines (2nd edition). Chest. 2007;132(3 Suppl):178S–201S.
37. Shim SS, Lee KS, Kim BT, Chung MJ, Lee EJ, Han J, et al. Non-small cell lung cancer: Prospective comparison of integrated FDG PET/CTand CT alone for preoperative staging. Radiology. 2005;236:1011–9.
38. Kim SK, Shin JE, Lee JH. Peripheral tuberculous lymphadenitis masquerading as metastatic gastric carcinoma on F-18 FDG dual time point PET/CT. Nucl Med Mol Imaging. 2012;46:316–7.
39. Kim YK, Lee KS, Kim BT, Choi JY, Kim H, Kwon OJ, et al. Mediastinal nodal staging of non small cell lung cancer using integrated FDG PET/CT in a tuberculosis-endemic country. Cancer. 2007;109:1068–77.